Overhauser shift of the electron spin-resonance line of Si:P at the metal-insulator transition: I. Integral shift

2001 J. Phys.: Condens. Matter 13 10065

(http://iopscience.iop.org/0953-8984/13/44/318)

INSTITUTE OF PHYSICS PUBLISHING JOURNAL OF PHYSICS: CONDENSED MATTER

J. Phys.: Condens. Matter **13** (2001) 10065–10075 PII: S0953-8984(01)26234-1

Overhauser shift of the electron spin-resonance line of Si:P at the metal–insulator transition: I. Integral shift

Ulrike Fasol and Elmar Dormann

Physikalisches Institut, Universität Karlsruhe (TH), 76128 Karlsruhe, Germany

Received 27 July 2001, in final form 28 September 2001
Published 19 October 2001
Online at stacks.iop.org/JPhysCM/13/10065

Abstract

The shift of the electron spin-resonance (ESR) line caused by a dynamic nuclear spin polarization is measured at low temperatures (5–11 K) and X-band frequency for phosphorus-doped silicon in the concentration range (2.7–7.3) $\times 10^{18}$ cm^{-3} covering the metal–insulator transition. The samples are also characterized by the temperature dependence of their microwave electrical conductivity. The g-factor, ESR linewidth and saturation behaviour are analysed as regards their dependence on the temperature and phosphorus concentration. The variation of the integral Overhauser shift of the ESR line with the temperature and phosphorus concentration is derived and discussed.

1. Introduction

Phosphorus occurs as a substitutional donor in silicon with a weakly bound electron. The wave-function of such electrons is spread over several lattice constants. Samples with low P concentration are insulators at low temperatures. If the P concentration is higher than a critical concentration ($N_c = 3.52 \times 10^{18}$ cm^{-3} [1]) the crystals become metallic. The accompanying changes of the electronic structure can be monitored by means of the magnetic resonance. The isotropic hyperfine interaction (Fermi-contact interaction) is proportional to the electron density at the nucleus. Feher [2] used the classical electron–nuclear double-resonance (ENDOR) technique to obtain information about the hyperfine interaction of the isolated donor electron with the ^{29}Si ($I = 1/2$) nuclei situated at different lattice sites. The P concentration of the sample was $N = 5 \times 10^{16}$ cm^{-3}, which is two orders of magnitude smaller than N_c. At P concentration higher than about 1×10^{18} cm^{-3}, which is still lower than N_c, the exchange interaction between nearest-neighbour electron spins is so large that most of the electron spins are no longer localized at one P atom. As a result, in electron spin-resonance (ESR) experiments, only one line is observed instead of the two lines at low P concentration which are split by the hyperfine interaction with the ^{31}P nuclei ($I = 1/2$). Since there are not as many nuclear spins parallel as antiparallel to the external magnetic field, the electron spins still experience an average non-zero hyperfine field, but at thermal equilibrium this is at 5 K at least seven orders of magnitude smaller than the external magnetic field used for

the experiment (about 3500 G). The nuclear Zeeman interaction is about a factor of 2000 smaller than that of the electron spin. For that reason it should be possible to observe a shift of the nuclear magnetic resonance (NMR) line due to the hyperfine interaction (paramagnetic shift or Knight shift). Several groups performed standard NMR experiments using the ^{29}Si nuclear spins in Si:P (natural abundancy 4.7%; ^{28}Si and ^{30}Si have no nuclear spin). In the vicinity of N_c the ratio of P atoms to Si atoms is about 1:14 000. For this reason only a very small proportion of the Si nuclear spins experience a measurable hyperfine interaction and the NMR spectrum is dominated by the Si bulk. On the other hand, this means that the number of ^{31}P nuclear spins (natural abundancy 100%) in the sample is very small, which results in a very small and hardly detectable NMR signal of P nuclear spins. So far there have been few publications on this, and only Alloul and Dellouve [3] have published results on standard NMR experiments using P nuclear spins with P concentration in the vicinity of N_c and below N_c.

The Overhauser shift is a shift of the ESR line caused by an enhanced hyperfine field. If the ESR transition is partly saturated, the nuclear spin polarization is strongly increased by the so-called Overhauser effect [4]. The resonance condition for electron spins is given by

$$h\nu = g\mu_B B_{total} = g\mu_B(B_0 + B_{HF}). \tag{1}$$

In continuous-wave experiments the frequency ν is stabilized to the resonance frequency of the cavity and the external static magnetic field (B_{ext}) is swept. B_{HF} is the internal field caused by nuclear spin polarization. For thermal polarization of the nuclear spins, the ESR line will be found at $B_{ext} = B_0$. If the nuclear spin polarization is increased by the Overhauser effect, B_{HF} changes, and as a result B_0 also, which means that the ESR line is shifted. This is only possible for a system where the electron spins are exchange coupled or mobile and so have a single homogeneous resonance line. For these systems a standard ENDOR experiment can no longer be performed. If the ESR of Si:P samples with P concentration in the vicinity of N_c is partly saturated, the P nuclear spin polarization and the polarization of the Si nuclear spins near to the P atoms are enhanced. The resulting shift of the ESR line is the integral over the effects caused by Si and P nuclear spins. To separate the Overhauser shift caused by the P nuclear spins from that caused by the Si nuclear spins it is necessary to destroy the polarizations separately [5, 6]. This is possible because the NMR frequencies are different ($\nu_P/\nu_{Si} \approx 2$).

In the current investigation, Si:P samples with $N = (2.7\text{–}7.3) \times 10^{18}$ cm^{-3} have been surveyed at 5–11 K. The sample preparation is described in the next section. In the third section of this paper the samples will be characterized by the microwave conductivity. In section 4 the standard ESR parameter linewidth and g-factor will be described. The integral Overhauser shift of the ESR line will be discussed in section 5. The results on the separated Overhauser shifts caused by ^{29}Si and ^{31}P nuclear spins will be published at a later date.

2. Sample preparation and experimental details

Samples were cut out of large Czochralski-grown single crystals with a P concentration gradient of $N^{-1}(\Delta N/\Delta x) = 10^{-2}$ cm^{-1} along the axis of the rods. The P concentration of the samples with $N = 2.7 \times 10^{18}$ and 7.3×10^{18} cm^{-3} was determined from the room temperature resistivity using the calibration of Thurber *et al* [7]. A more accurate (relative) determination of N was obtained from the ratio of the resistances at 4.2 K and 296 K where the uncertainties of the sample geometry could be eliminated [8]. After determination of the P concentration, small flat samples of area $\approx$1.3–3.4 mm^2 and thickness 0.025–0.081 mm ($\leqslant$skin depth at 5–11 K for 9.8 GHz) were prepared. To get clean surfaces without additional ESR signals the

samples were etched with a mixture of HNO_3, HF and acetic acid (*pro analysi*, 5:3:3). The samples are labelled according to their P concentration; e.g. N5.1.3 is the third of the samples with P concentration 5.1×10^{18} cm^{-3}.

For the ESR experiments an X-band Bruker ESP300E spectrometer with a dielectric cavity and an Oxford Instruments cryostat were used. For more experimental details see [9].

3. Microwave conductivity

The temperature dependence of the microwave conductivity at 10 GHz is shown in figure 1. The values are normalized to the high-temperature conductivity. The dependence of the conductivity on decreasing temperature shows clearly the change from semiconducting to metallic behaviour with increasing P concentration.

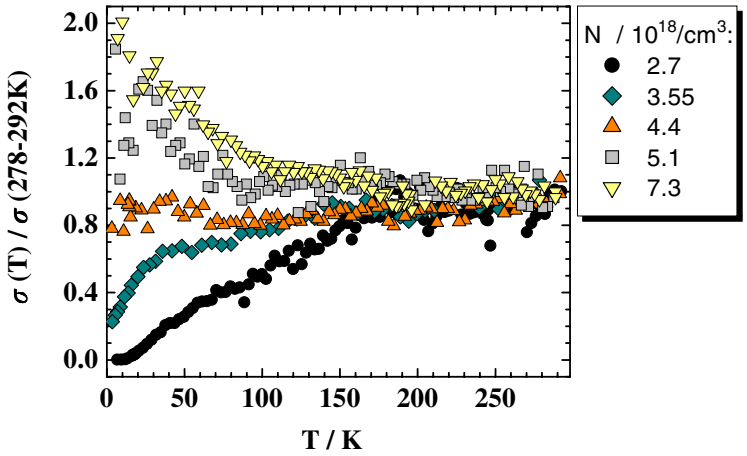

Figure 1. Microwave conductivity of Si:P versus temperature for the five doping levels used for the current analysis. The microwave conductivity was determined at 10 GHz by applying the cavity perturbation technique [10] and normalized to the high-temperature values.

4. ESR *g*-factor, linewidth and saturation behaviour

Although the thicknesses of the samples were less than the skin depth, the ESR lines of the samples with $N = 3.55$, 4.4, 5.1 and 7.3×10^{18} cm^{-3} were at least slightly asymmetric (see figure 2). Pifer [12] showed that the ESR line for conducting samples becomes symmetric again only when the ratio of the skin depth to the sample thickness $\rightarrow\infty$. The asymmetry is caused by the phase shift and damping of the microwave field on its way through the conductive crystal plates. A so-called Dysonian line [11] can be calculated analytically for special cases depending on spin-relaxation times, the diffusion constant and the mobility of the electrons. Since these quantities are not known exactly for our samples and since the current analysis is focused on the shift of the ESR line caused by nuclear spin polarization, the ESR spectra were fitted with the derivative of a superposition of absorption and dispersion parts of a Lorentzian line to get the appropriate line position and width. Thus only an average value of the width and phase is considered, but the fit is fully satisfactory as is illustrated in figure 2. The relative

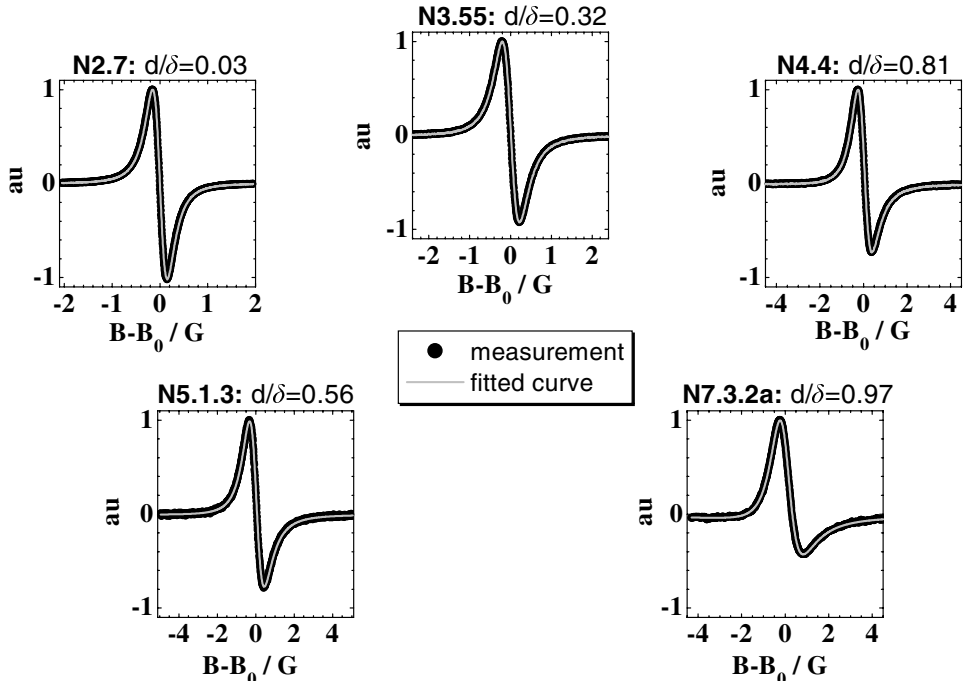

Figure 2. ESR lines of different Si:P samples at 5.2–5.5 K. A smaller ratio of sample thickness (d) to skin depth (δ) results in a more symmetric line. The fitted curves (grey) describing each of these lines as the derivative of superimposed absorption and dispersion parts of a Lorentzian line are shown in comparison to the measurement (black).

weight of absorption and dispersion was a parameter of the fit and it changes according to the asymmetry of the ESR lines. The comparison of results for different samples with the same P concentration but different thickness shows that the error in determining the linewidth is less than 6%. The linewidth is given as the halfwidth at half-amplitude of the resulting absorption part, and the g-factor is calculated from the resulting resonance field.

The change of the g-factor and linewidth of the current samples with the P concentration and temperature (5–11 K) are shown in figures 3(a)–3(d). The g-factor increases with increasing P concentration from $N = 2.7 \times 10^{18}$ cm^{-3} to 5.1×10^{18} cm^{-3} within the accuracy of the measurement, (a), and with increasing temperature in the surveyed region (5–11 K), (b). The linewidth shows a minimum between 2×10^{18} cm^{-3} and 3.55×10^{18} cm^{-3}, (c). The results from earlier publications are also shown for comparison in this diagram. With increasing temperature, from 5 to 11 K, the linewidth increases, (d). The results essentially correspond with the results from earlier publications [12–23] and we refer the reader to these references for a detailed discussion. The ESR lines of the samples with $N = 2.7 \times 10^{18}$ cm^{-3} and 3.55×10^{18} cm^{-3} become more asymmetric with increasing saturation, which cannot be explained by just the effect of the saturation on a single ESR line. This behaviour of the lineshape decreases from $N = 2.7 \times 10^{18}$ cm^{-3} to 3.55×10^{18} cm^{-3} and is no longer observed for $N \geqslant 4.4 \times 10^{18}$ cm^{-3}. It can be explained by regions with different hyperfine interactions in the samples, which do not exchange electron spins. This is possible due to the random distribution of the P atoms in the crystal and the low P concentration.

The saturation of the ESR depends on the longitudinal (τ_1) and the transverse (τ_2) relax-

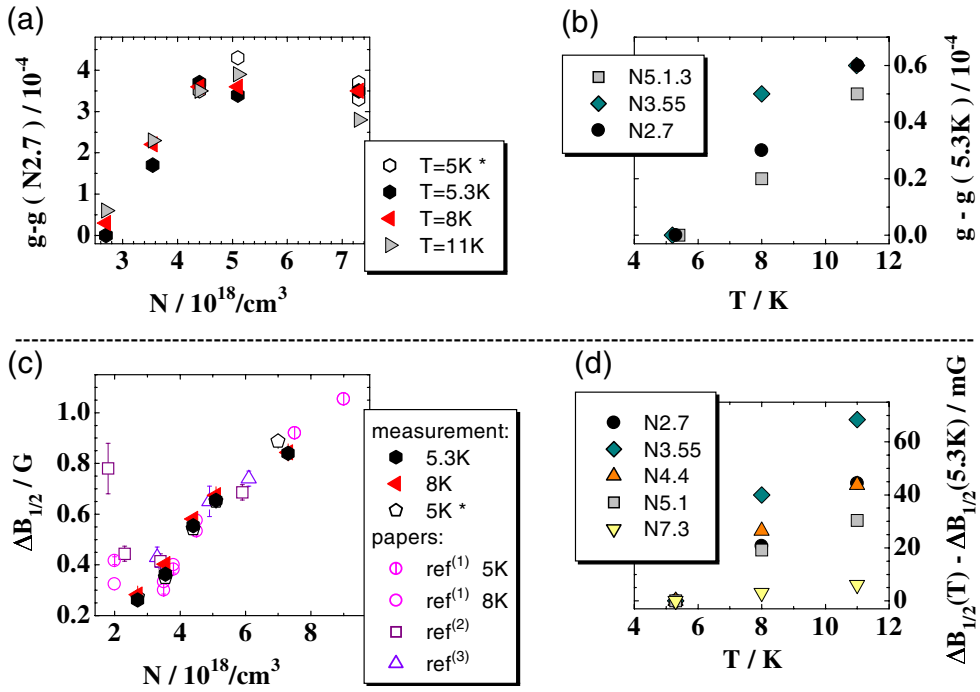

Figure 3. Changes of the g-factor ((a), (b)) and of the linewidth ((c), (d)) with P concentration ((a), (c)) and temperature ((b), (d)). The accuracy of the g-factor change is (6–8) $\times 10^{-5}$. Some linewidth data reported in the literature are also shown for comparison in graph (c) ('ref$^{(1)}$': [12]; 'ref$^{(2)}$': [16]; 'ref$^{(3)}$': [14]). (The asterisks mark results of initial experiments.)

ation times of the electron spins and on the amplitude of the microwave magnetic field strength (B_1). Usually B_1 is not known exactly and instead the power (P_{ESR}) is given. According to Abragam [24], the saturation factor can be written as

$$s = \frac{S_0 - \langle S_z \rangle}{S_0} = \frac{\gamma_e^2 B_1^2 \tau_1 \tau_2}{1 + \gamma_e^2 B_1^2 \tau_1 \tau_2} = \frac{\alpha P_{ESR}}{1 + \alpha P_{ESR}} \tag{2}$$

with S_0 the thermal equilibrium and $\langle S_z \rangle$ the actual average value of the electron spins' z-component. γ_e is the gyromagnetic ratio of the electron spins and α the so-called saturation parameter. In addition to depending on the relaxation times, it also depends on how well the power is fed into the cavity. This is influenced by the experimental set-up and the quality factor of the cavity including the probe-head and sample. If the ESR is partly saturated, the Lorentzian line is given by

$$\chi'' \propto \frac{\Delta B_{1/2}}{(\Delta B_{1/2})^2 (1 + \alpha P_{ESR}) + (B - B_0)^2} \tag{3}$$

where $\Delta B_{1/2} = 1/(\gamma_e \tau_2)$ is the halfwidth at half-amplitude of an unsaturated line and B_0 is the resonance field (static). For each sample studied, α was determined by taking the ESR spectra at different ESR powers and fitting them with equation (3) and the corresponding dispersion component. The linewidth ($\Delta B_{1/2}$) and the proportion of absorption to dispersion was given by the results of the measurement without saturation.

The results for the saturation parameter are shown in figure 4(a). The fluctuations of the α-value within the measurements for one sample and at one temperature are 1–6%. For

$N = 5.1 \times 10^{18}$ cm^{-3} and 7.3×10^{18} cm^{-3} two samples with different sizes have been analysed. As could be expected from the decrease of the linewidth with decreasing P concentration in the observed region, the power needed to reach the same saturation factor decreases with decreasing P concentration. Knowing the saturation parameter (α) for each sample and temperature, the saturation factor (s) can be calculated for each ESR power.

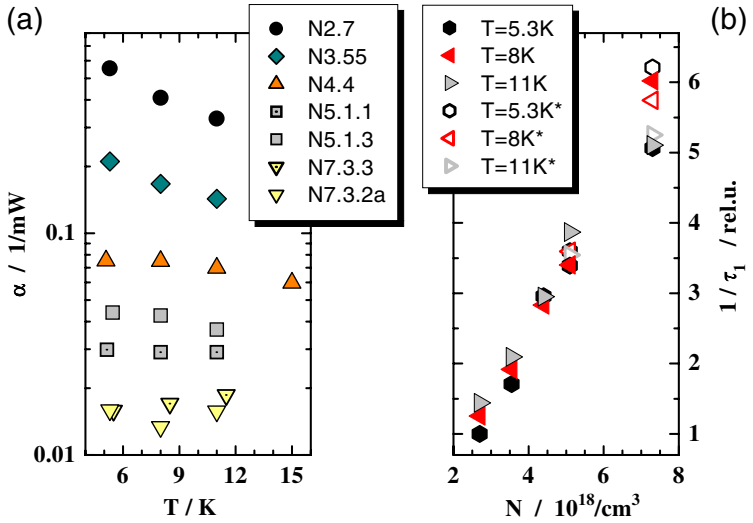

Figure 4. The variation of the ESR saturation parameter with temperature for different samples (a) and the longitudinal relaxation rate of the electron spins, as calculated from the saturation parameter with the help of the quality factor of the cavity and the ESR linewidth (b). (Asterisks: N5.1.1 and N7.3.3).

The quality factor (Q) of the loaded and coupled cavity can easily be determined with the spectrometer. So it is possible to get a value which is proportional to the longitudinal relaxation rate:

$$\frac{1}{\tau_1} = C\frac{Q}{\alpha\,\Delta B_{1/2}}. \tag{4}$$

Q is the quality factor of the cavity with the probe-head and the sample, and C is a constant depending only on the device. In figure 4(b) the dependence of the relaxation rate on the P concentration is shown. Similarly to the linewidth (figure 3), which is proportional to the transverse relaxation rate, the longitudinal relaxation rate increases with increasing P concentration in the observed region. This behaviour continues the dependence of the longitudinal relaxation rate for samples with $N = 3.85 \times 10^{16}$ cm^{-3}–1.7×10^{18} cm^{-3} published by Maekawa and Kinoshita [25].

5. Integral Overhauser shift

The derivation of the Overhauser shift is the primary target of the current investigation. As described in the introduction, the ESR line is shifted by the hyperfine field of the dynamically polarized nuclear spins (equation (1)). By fitting the ESR spectra with a Lorentzian line (equation (3)) the line position B_0 is derived. B_0 is about 3500 G ($\nu \approx 9.8$ GHz). The change of B_0 with increasing ESR saturation is the integral Overhauser shift. For each sample a small saturation ($s_0 \neq 0$) was chosen, which was part of each measurement series at 5, 8 and 11 K.

The shift originally derived is the change of the ESR position in comparison to the position at the chosen saturation s_0. However, in figure 5 and figure 6 (N2.7, N3.55 and N4.4), we plotted these data relative to the value at the smallest saturation $s \to 0$, so that the change of the slope according to the P concentration or temperature can be observed more readily. Most of the measurement series have been performed more than once and the deviations are very small.

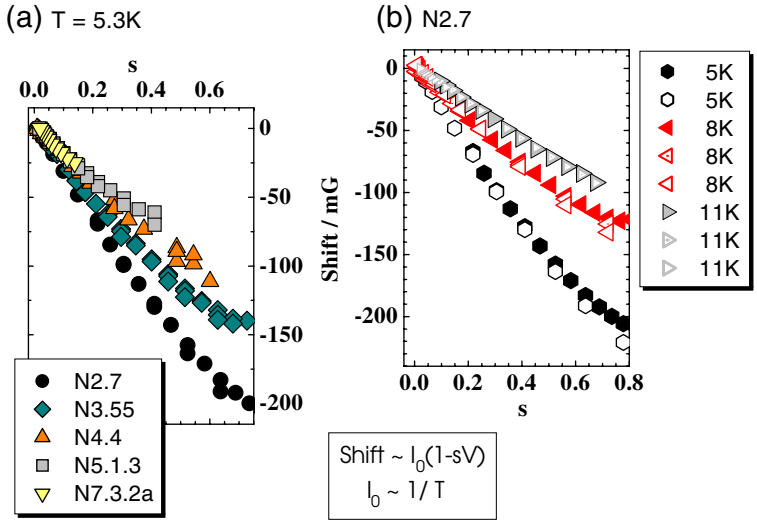

Figure 5. Integral shift of the ESR line as a function of the ESR saturation: (a) for different P concentrations at 5.3 K and (b) for $N = 2.7 \times 10^{18}$ cm^{-3} at different temperatures.

For all samples and temperatures the ESR line is shifted to smaller fields B_0 with increasing saturation. This means that the dominating hyperfine field has a positive sign. The additional field caused by the isotropic hyperfine interaction of one type i of nuclear spin (characterized by their gyromagnetic ratio $\gamma_n = \gamma_{\mathrm{Si}}$ or γ_{P} respectively and the type and strength of their interactions [24]) is given by

$$(B_{HF})_i = (B^0_{HF})_i(1 - sV_i). \tag{5}$$

B^0_{HF} is the hyperfine field at thermal equilibrium ($B^0_{HF}/B_0 \approx 1 \times 10^{-7}$), s is the ESR saturation factor and $V = f\gamma_e/\gamma_n$ is the amplification factor with the leakage rate $0 < f \leqslant 1$ [6]. If the isotropic (Fermi-contact) hyperfine interaction is the dominating interaction for the nuclear spins, there is no leakage of polarization and $|V| = |\gamma_e/\gamma_n|$. If the nuclear spins have an alternative relaxation path, the polarization that can be reached is smaller and $|V| < |\gamma_e/\gamma_n|$. Since $\gamma_e < 0$, $\gamma_{\mathrm{Si}} < 0$ and $\gamma_{\mathrm{P}} > 0$, the amplification factor of Si nuclear spins is $V_{\mathrm{Si}} > 0$ and that of P nuclear spins is $V_{\mathrm{P}} < 0$. If the amplified nuclear spin polarization is built up by the anisotropic (dipolar) hyperfine interaction, the sign of the polarization and that of the Overhauser shift are inverted. The maximum possible amplification factor is in this case $|V| = 0.5|\gamma_e/\gamma_n|$. However, our results support a dominant isotropic hyperfine interaction.

The respective importance of the ^{31}P and ^{29}Si nuclei must be discerned, but the predominance of the ^{31}P contribution can be verified. The integral Overhauser shift is the integral over the effects caused by the polarization of both types of nuclear spin. The sign of the shift shown in figure 6 and figure 5 is negative, which is a result of an increasing positive hyperfine field. This means that the hyperfine field of the P nuclear spins dominates the integral shift, since we can assume that at least for $N \leqslant 3 \times 10^{18}$ cm^{-3} the dominating hyperfine interaction

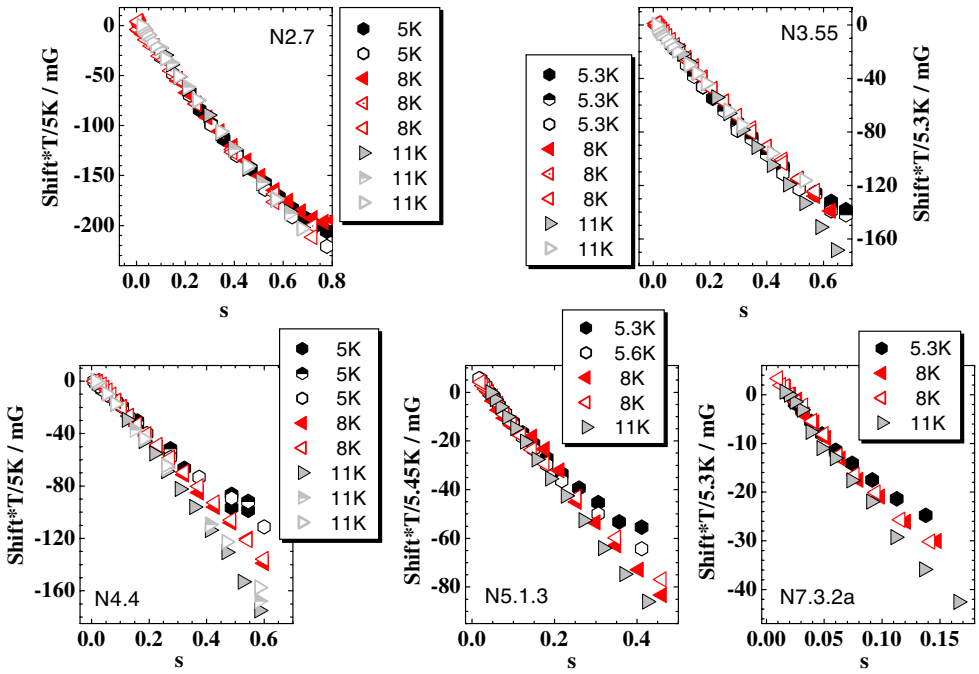

Figure 6. Integral shift of the ESR line as a function of the ESR saturation for each P concentration at different temperatures. The values are multiplied by the ratio temperature $T/5$ K to demonstrate the adherence to the Curie law of the nuclear spin polarization in thermal equilibrium.

is the Fermi-contact interaction [5, 26]. The unpaired electron spins for the ESR are those of the weakly bound electrons of the P atoms. Since the natural abundance of ^{31}P is 100%, each electron spin experiences, in the P concentration range analysed, mainly the hyperfine field of one P nuclear spin. Between the P atoms there are a large number of Si atoms, but the natural abundance of ^{29}Si is only 4.7%. The isotropic hyperfine interaction is proportional to the electron density at the nucleus. Since the weakly bound electron is supposed to have a hydrogen-like wave-function with a radius $a_B \approx 17$ Å [27], the electron density at the P nucleus is larger than that at Si nuclei. On the other hand, there is more than one Si nucleus with spin per electron. Thus the balance must be struck quantitatively.

As mentioned before, Si:P samples with very low P concentrations, and therefore localized electrons, show a hyperfine splitting of ± 21 G in ESR experiments. The electron density at the P nucleus calculated from this splitting is

$$|\Psi(0)|^2 = 21\ \mathrm{G} \times \frac{3}{8\pi}\frac{1}{\hbar\gamma_\mathrm{P}}\frac{1}{1/2} \approx 4.4 \times 10^{23}\ \mathrm{cm}^{-3}.$$

For this electron density the hyperfine field caused by P nuclear spins for the electron spins in thermal equilibrium is then B^0_{HF}(phosphorus) ≈ 0.61 mG. The highest possible amplification for P is $V_\mathrm{P} = -1622$. For a homogeneous crystal without Si nuclear spins the ESR would then be shifted at 5 K and e.g. $s = 0.7$ by -693 mG. To estimate the shift caused by the Si nuclear spins, it is necessary to sum up the interactions with all Si nuclear spins in the neighbourhood of a P atom. The spatial variation of the respective contributions to the Overhauser shift of the ESR line was analysed in detail [9]. In order to estimate the range of possible Si-induced shift values we proceed as follows. We used a hydrogen-like wave-function centred at the P atom,

with radius $a_B = 17$ Å [27]. The amplitude is chosen in such a way that it causes the hyperfine interaction at respective Si lattice points to agree with the results of Feher [2]. It can easily be shown that the contribution of Si nuclear spins which are more than about 80 Å away from the next P atom can be neglected [9]. Taking all Si nuclear lattice points within a sphere of radius 80 Å into account, with a maximum possible amplification of $V_{\mathrm{Si}} = 3305$, and the natural abundance 4.7% of ^{29}Si, the Overhauser shift caused by the Si nuclear spins at saturation with $s = 0.7$ and $T = 5$ K adds up to $\approx$+562 mG. This yields an integral shift due to ^{31}P and ^{29}Si of -693 mG+562 mG $= -131$ mG. Since the hyperfine interaction between the Si nuclear spins and the electron spin decreases rapidly with the distance between the Si nucleus and the next P atom due to the exponential decrease of the electron density, the time constant for building up the dynamical nuclear spin polarization increases with distance [24]. For this reason, it is very likely that only the Si nuclear spins within a certain radius $r < 80$ Å are of relevance. Taking as an extreme example only the Si nuclear spins within a sphere of radius $r = 25$ Å into account, the corresponding ^{29}Si part of the shift would be $\approx$+446 mG. The integral shift would then be -247 mG. The estimated values of -131 to -247 mG for $s = 0.7$ and $T \approx 5$ K are evidently comparable to the experimental results shown in figure 5(a).

These estimates are for a homogeneous system, whereas we know that the current samples are not homogeneous: the P atoms are statistically distributed [28]. We know that there exists exchange coupling between electron spins which can change the form of the wave-function. Furthermore, both amplification factors V_{P} and V_{Si} can be reduced by a leakage rate. The distance from the P atom at which the Si nuclear spins no longer have significant influence and where the time constant of the dynamical polarization can have an influence on the measurement is not known. Nevertheless, the agreement of estimated and measured integral Overhauser shifts is persuasive.

Figure 5(a) shows the integral shift at 5.3 K for varied P concentration. From $N = 2.7 \times 10^{18}$ cm^{-3} to 4.4×10^{18} cm^{-3} the slope decreases significantly. A further change from $N = 4.4 \times 10^{18}$ cm^{-3} to 7.3×10^{18} cm^{-3} is not detectable within the precision of the determination. The change of the slope for varied temperature is shown for $N = 2.7 \times 10^{18}$ cm^{-3} in figure 5(b). For both sorts of hyperfine interaction the mean nuclear spin polarization at thermal equilibrium, I_0, is given by the Curie law and therefore $B^0_{HF} \propto 1/T$. The slope of the integral shift with increasing ESR saturation decreases for all samples with increasing temperature. Figure 6 shows the shift for five samples with different P concentration. The values are multiplied by $T/5$ K to check whether just the Curie law for I_0 is responsible for the temperature dependence.

For $N = 2.7 \times 10^{18}$ and 3.55×10^{18} cm^{-3} the agreement with the Curie law is perfect. The samples with higher P concentration show a slight deviation. As mentioned before, a possible explanation for this is that, for higher P concentration, the leakage rate also depends on the temperature. So the temperature dependence of the shift of the ESR line can be understood in the framework of equation (5).

6. Conclusions

We have analysed the low-temperature ESR and derived the integral Overhauser shift of the ESR line for a set of Si:P samples with P concentration varying from below to above the critical concentration N_c of the metal–insulator transition. Line shifts of 4×10^{-4} to 0.8 times the linewidth are observed. The change of the ESR lineshape with increasing saturation of the samples with $N = 2.7 \times 10^{18}$ cm^{-3} and 3.55×10^{18} cm^{-3} shows that at these P concentrations there are still different regions in the sample whose electron spins do not communicate with each other. The Overhauser shift was derived as a function of ESR saturation and temperature. The

resulting hyperfine field is positive: the ESR line shifts to lower external field with increasing saturation. The slope of the integral shift, depending on the ESR saturation, decreases from $N = 2.7 \times 10^{18}$ cm^{-3} to 4.4×10^{18} cm^{-3} at 5.3 K, but no further change of the slope with further increasing P concentration is observed within the accuracy of the current determination. This difference of slopes can be caused by a change of the wave-function of the electron and therefore of B^0_{HF} for the Si and P nuclear spins. But it is also possible that the leakage rates of Si and P nuclear spins change, which results in different amplification factors V_{Si} and V_{P}. Nevertheless, it is possible to estimate the shift caused by P and Si nuclear spins for a simplified situation: the estimated values of -131 to -247 mG for $s = 0.7$ and $T = 5$ K are of the same order of magnitude as the results of the measurement.

The integral Overhauser shift shows the temperature dependence that is caused by the Curie-like behaviour of the nuclear spin polarization at thermal equilibrium. For $N \geqslant 4.4 \times 10^{18}$ cm^{-3} the influence of an additional temperature-dependent process is observed. Again, the leakage rate of the dynamical nuclear polarization is a possible candidate for providing an explanation.

Interpretation of the total shift is non-trivial. First of all, the sign of the shift of the ESR line caused by the Si nuclear spin polarization is opposite to that caused by the P nuclear spins. Furthermore, the dynamical nuclear polarization that is built up by the isotropic hyperfine interaction has the opposite sign to that which would be built up via an anisotropic (dipolar) hyperfine interaction. Thus, only under the reasonable assumption that the isotropic hyperfine interaction is responsible for the Overhauser shift of the ESR line in Si:P can it be concluded that the integral shift is dominated by the P nuclear spin polarization. It is necessary to determine the shift caused by Si and P nuclear spins separately in order to obtain more information about the type of hyperfine interaction and its distribution among the nuclear spins. The time constant of the dynamical polarization can give further information on the hyperfine interaction. The results of NMR-frequency-resolved Overhauser shift measurements and the respective time constants will be published at a later date.

Acknowledgments

We thank Professor H von Löhneysen for providing the samples, S Waffenschmidt for the determination of the P concentration and B Pongs for the measurements of the microwave conductivity. This work was financially supported by the Deutsche Forschungsgemeinschaft within the Sonderforschungsbereich 195 (Universität Karlsruhe).

References

[1] Stupp H, Hornung M, Lakner M, Madel O and von Löhneysen H 1993 *Phys. Rev. Lett.* **71** 2634
[2] Feher G 1959 *Phys. Rev.* **114** 1219
[3] Alloul H and Dellouve P 1987 *Phys. Rev. Lett.* **59** 578
[4] Overhauser A W 1953 *Phys. Rev.* **92** 411
[5] Jerome D, Ryter Ch and Winter J M 1965 *Physics* **2** 81
[6] Denninger G 1990 *Festkörperprobleme (Advances in Solid State Physics)* vol 30 (Braunschweig: Vieweg) p 113
[7] Thurber W R, Mattis R L, Liu Y M and Filliben J J 1980 *J. Electrochem. Soc.* **127** 1807
[8] Rosenbaum T F, Andres K and Thomas G A 1980 *Solid State Commun.* **35** 663
[9] Fasol U 2001 Messung der Overhauserverschiebung an Si:P im Bereich des Metall–Isolator-Übergangs *PhD Thesis* Physikalisches Institut, Universität Karlsruhe (TH) (Aachen: Shaker)
[10] Helberg H W and Wartenberg B 1966 *Z. Angew. Phys.* **20** 505
[11] Dyson F J 1955 *Phys. Rev.* **98** 349
[12] Pifer J H 1975 *Phys. Rev.* B **12** 4391
[13] Maekawa S and Kinoshita N 1965 *J. Phys. Soc. Japan* **20** 1447

[14] Ue H and Maekawa S 1971 *Phys. Rev.* **3** 4232
[15] Quirt J D and Marko J R 1972 *Phys. Rev.* B **5** 1716
[16] Quirt J D and Marko J R 1973 *Phys. Rev.* B **7** 3842
[17] Ochiai Y and Matsuura E 1976 *Phys. Status Solidi* a **38** 243
[18] Swarup P and Trivedi P L 1976 *Sov. Phys.–Solid State* **18** 190
[19] Gershenzon E M, Semenov I T and Fogel'son 1984 *Sov. Phys.–Semicond.* **18** 263
[20] Paalanen M A, Sachdev S, Bhatt R N and Ruckenstein 1986 *Phys. Rev. Lett.* **54** 1295
[21] Stesmans A 1987 *Phys. Status Solidi* b **143** 733
[22] Zarifis V and Castner T G 1987 *Phys. Rev.* B **36** 6198
[23] Mason P J and Tunstall D P 1991 *J. Phys.: Condens. Matter* **3** 8095
[24] Abragam A 1982 *Principles of Nuclear Magnetism* (Oxford: Clarendon)
[25] Maekawa S and Kinoshita N 1964 *J. Phys. Soc. Japan* **19** 2240
[26] Dyakonov V and Denninger G 1992 *Phys. Rev.* B **46** 5008
[27] Cullis P R and Marko J R 1970 *Phys. Rev.* B **1** 632
[28] Trappmann T, Sürgers Ch and von Löhneysen H 1997 *Europhys. Lett.* **38** 177